Running title: Construction of reversed methylotrophy in *E. coli*

Methanol production by reversed methylotrophy constructed in *Escherichia coli*

Tomoyuki Takeya, Miyabi Yamakita, Daisuke Hayashi, Kento Fujisawa, Yasuyoshi Sakai, and Hiroya Yurimoto*

Division of Applied Life Sciences, Graduate School of Agriculture, Kyoto University, Kitashirakawa-Oiwake, Sakyo-ku, Kyoto 606-8502, Japan

*Correspondence: Hiroya Yurimoto, Division of Applied Life Sciences, Graduate School of Agriculture, Kyoto University, Kitashirakawa-Oiwake, Sakyo-ku, Kyoto 606-8502, Japan. Tel.: +81 75 753 6387; Fax: +81 75 753 6454; E-mail: yury@kais.kyoto-u.ac.jp

Abstract

We constructed a reversed methylotrophic pathway that produces methanol, a promising feedstock for production of useful compounds, from fructose 6-phosphate (F6P), which can be supplied by catabolism of biomass-derived sugars including glucose, by a synthetic biology approach. Using *Escherichia coli* as an expression host, we heterologously expressed genes encoding methanol utilization enzymes from methylotrophic bacteria, i.e., the NAD^+-dependent methanol dehydrogenase (MDH) from *Bacillus methanolicus* S1 and an artificial fusion enzyme of 3-hexulose-6-phosphate synthase and 6-phospho-3-hexuloisomerase from *Mycobacterium gastri* MB19 (HPS-PHI). We confirmed that these enzymes can catalyze reverse reactions of methanol oxidation and formaldehyde fixation. The engineered *E. coli* strain co-expressing MDH and HPS-PHI genes produced methanol in resting cell reactions not only from F6P but also from glucose. We successfully conferred reversed methylotrophy to *E. coli* and our results provide a proof-of-concept for biological methanol production from biomass-derived sugar compounds.

Keywords

methanol dehydrogenase, 3-hexulose-6-phosphate synthase, ribulose monophosphate pathway, *Bacillus methanolicus*, *Mycobacterium gastri*

Introduction

Much attention has been paid to methanol as an alternative carbon resource to replace fossil fuels, because methanol can be derived from various carbon sources including methane, CO_2, and biomass, and is a key organic chemical used in the production of many kinds of chemicals, plastic materials and other value-added products [1]. In the field of bioindustry, methanol is not only a carbon source for microbial fermentation processes, but also a substrate for biological production of industrial chemicals [2-4]. To date, a variety of methods for methanol production via chemical processes have been developed [1], however, no biological production processes for methanol from biomass constituents such as sugar compounds, that is analogous to bioethanol production, are currently available. Construction of a synthetic biological pathway in a heterologous host using enzymes involved in the metabolism of one-carbon (C1) compounds including methanol can be a possible solution to establish a metabolic pathway that produces methanol from biomass-derived sugar compounds.

Methylotrophic bacteria, which can use methanol as the sole carbon and energy source, have diverse types of methanol metabolic pathways. Methanol is first oxidized to formaldehyde by methanol dehydrogenases (MDHs). Gram-negative methylotrophic bacteria possess MDHs that require pyrroloquinoline quinone (PQQ) as a cofactor [5]. In contrast, gram-positive methylotrophic bacteria possess $NAD(P)^+$-dependent MDHs [6]. For example, the thermophilic methylotroph *Bacillus methanolicus* possesses an NAD^+-dependent MDH and this type of MDH requires the activator protein Act for efficient methanol oxidation *in vitro* [7].

Formaldehyde produced by MDH next undergoes further oxidation to CO_2 or fixation to cell constituents. The two major assimilatory pathways in methylotrophic

62 bacteria are the serine pathway and the ribulose monophosphate (RuMP) pathway [8].
63 In the bacteria which use serine pathway for formaldehyde assimilation, the
64 incorporation of a C1 unit into serine involves the tetrahydromethanopterin (H_4MPT)-
65 and glutathione-dependent oxidation of formaldehyde to formate, the conjugation of
66 formate and tetrahydrofolate (H_4F) to produce 5,10-methylene-H_4F, and the transfer of
67 the C1 unit of 5,10-methylene-H_4F to glycine. On the other hand, in the RuMP pathway,
68 formaldehyde is fixed to ribulose 5-phosphate (Ru5P) by 3-hexulose-6-phosphate
69 synthase (HPS), forming D-*arabino*-3-hexulose 6-phosphate (Hu6P), which is then
70 isomerized to fructose 6-phosphate (F6P) by 6-phospho-3-hexuloisomerase (PHI) [9].
71 Recent studies have engineered model bacterium including *Escherichia coli* to
72 incorporate methanol by introducing the enzymes for C1 metabolism [10-15]. These
73 studies have usually employed NAD^+-dependent MDH, HPS and PHI for their ease of
74 functional production in the host species, because these enzymes do not require any
75 methylotrophy-specific cofactors (PQQ, H_4MPT and H_4F), and the substrate Ru5P and
76 the product F6P exist in almost all organisms, enabling coupling to the endogenous
77 pentose phosphate pathway.
78 Theoretically, the reverse reactions of methanol oxidation and formaldehyde
79 fixation by MDH, HPS and PHI should result in the production of methanol from F6P,
80 which can be derived from sugar compounds (Figure 1). In fact, it has been reported
81 that the NAD^+-dependent MDH catalyzes the reverse reaction (i.e., reduction of
82 formaldehyde to methanol), which does not require the activator protein Act [16], and
83 the fused form of HPS and PHI (HPS-PHI) found in some hyperthermophilic archaea
84 also catalyzes the reverse reaction (i.e., production of formaldehyde and Ru5P from
85 F6P) [9,17]. Here we describe the construction of a reversed methylotrophic pathway to

produce methanol from F6P or glucose in engineered *E. coli* cells that express genes encoding NAD^+-dependent MDH from *B. methanolicus* S1 (reclassified from *B. brevis* S1) [18,19], and the artificial fusion enzyme HPS-PHI, which was constructed with the *hps* and *phi* genes from *Mycobacterium gastri* MB19 [20]. To our knowledge, this would be the first report of the biotechnological use of the reverse reactions of C1 metabolism, and these results provide a starting point towards the industrially relevant biological supply of methanol from biomass sugars.

Materials and methods

Strains and culture conditions

E. coli strains used in this study are listed in Table 1. *E. coli* transformants were grown in Luria-Bertani (LB) medium at 37°C, to which 0.5 mM isopropyl-β-D-thiogalactopyranoside (IPTG) was added at mid-exponential phase (OD_{610} of 0.4-0.6), followed by overnight growth at 16°C to achieve an OD_{610} of 2-3. Ampicillin (50 μg/mL) and chloramphenicol (30 μg/mL) were added when applicable.

Plasmid construction

Plasmids used in this study are listed in Table 2. Oligonucleotide primers used in this study are listed in Table 3. The 1.1-kb *mdh* gene from *B. methanolicus* S1 excluding the stop codon was amplified by PCR from the genomic DNA. The 5'-end of each primer contained NheI or HindIII sites. This PCR product and the EcoRV-digested pBluescript II SK(+) were ligated to obtain pBSmdh. pETmdh-His was constructed by ligating the 1.1- and 3.6-kb NheI/HindIII fragments of pBSmdh and pET-23a(+). pDmH was constructed by inserting *mdh*-His_6 from pETmdh-His into the NcoI/EcoRI sites of

pETDuet-1. pDmHhp was constructed by inserting *hps-phi* from pEThps-phi [20] into the BglII/KpnI sites of pDmH. The expression vectors were introduced into *E. coli* Rosetta (DE3) by electroporation.

Preparation of cell-free extract

For purification of recombinant *B. methanolicus* S1 MDH tagged with 6xHis, IPTG-induced *E. coli* [pETmdh-His] cells were suspended in buffer A (50 mM potassium phosphate buffer (KPB, pH 7.5), 5 mM $MgSO_4$ and 1 mM dithiothreitol (DTT)) and then disrupted by French press (Constant cell disruption system one shot model, Constant Systems Ltd., UK). After centrifugation at 5,000 x *g* for 30 min at 4°C, the resulting supernatant was used as a cell-free extract. For preparation of a cell-free extract of IPTG-induced *E. coli* [pEThps-phi], and *E. coli* [pDmHhp], cells were suspended in buffer B (50 mM KPB (pH 6.5), 1 mM DTT, 0.1 mM phenylmethylsulfonyl fluoride (PMSF) and 5 mM $MgCl_2$), and disrupted by French press. After centrifugation at 10,000 x *g* for 10 min at 4°C, resulting supernatant was used as a cell-free extract.

Purification of recombinant B. methanolicus S1 MDH tagged with 6xHis

Cell-free extract (7.5 mL) was loaded onto 2 mL of column-packed Ni-NTA Agarose (QIAGEN, Hilden, Germany) preequilibrated with buffer C (57.5 mM NaH_2PO_4, 300 mM NaCl, pH adjusted to 8.0 with NaOH) containing 10 mM imidazole. The column was then washed twice with 2 column volumes of buffer C containing 20 mM imidazole. The column-bound protein was eluted with 2 mL of buffer C containing 250

mM imidazole. The eluted fraction was dialyzed against 50 mM KPB (pH 7.5) and used as purified MDH-His_6.

Protein analyses

Protein concentrations were determined using a Bio-Rad protein assay kit (Japan Bio-Rad Laboratories, Tokyo, Japan) with bovine serum albumin as the standard [21]. For sodium dodecyl sulfate polyacrylamide gel electrophoresis (SDS-PAGE), protein samples (10 μg) were mixed with 3X sample buffer (50 mM Tris-HCl pH 6.8, 30% (v/v) glycerol, 3% (w/v) SDS, 3% (v/v) 2-mercaptoethanol, a dash of bromophenol blue), boiled for 5 min and run on a 12% gel. For total protein staining, GelCode™ Blue Safe Protein Stain (Thermo Scientific, Waltham, MA) was used. For immunoblot analyses, proteins were transferred onto a PVDF membrane by semidry blotting (Bio-Rad, Richmond, CA). 6xHis-tagged proteins were detected using anti-His-tag mAb-HRP-DirecT (Medical & Biological Laboratories, Nagoya, Japan) at a 1:5,000 dilution and Western Lightning (Perkin-Elmer Life Science, Waltham, MA). HPS-PHI proteins were detected using rabbit anti-HPS antibody as described previously [20]. The signal was analyzed with LuminoGraph II (ATTO, Tokyo, Japan).

Enzyme assay

Formaldehyde reductase (FRD) activity was determined by following the formaldehyde-dependent oxidation of NADH as described previously [16]. The K_m and k_{cat} values of purified MDH-His_6 were determined using a Lineweaver-Burk plot of initial reaction velocity against different concentrations of the substrate formaldehyde. The activity of HPS-PHI to catalyze the forward reaction (F6P synthesis) was

157 determined by following the ribulose-5-phosphate-dependent production of F6P as
158 described previously [20] except that the formaldehyde and ribose 5-phosphate
159 concentrations were 2.5 mM. The activity of HPS-PHI to catalyze the reverse reaction
160 (formaldehyde production) was determined by following the F6P-dependent production
161 of formaldehyde as described previously [9] except that the reaction was performed at
162 30°C. One unit of activity was defined as the amount of enzyme that oxidized 1 μmol of
163 NADH (FRD reaction), produced 1 μmol of F6P (HPS-PHI forward reaction), or
164 produced 1 μmol of formaldehyde (HPS-PHI reverse reaction) per min. Each activity
165 value is presented as mean ± standard deviation (s.d.) of triplicate measurements.
166
167 ***Production of methanol by whole-cell reaction***
168 For production of methanol from formaldehyde, IPTG-induced *E. coli* [pETmdh-His]
169 and *E. coli* [pET-23a(+)] cells were suspended in 50 mM KPB (pH 6.7), 5 mM $MgSO_4$,
170 1 mM DTT and 10 mM formaldehyde, to achieve an optical density at 610 nm (OD_{610})
171 of 2.0, and incubated at 37°C. For production of methanol from F6P, IPTG-induced
172 cells of *E. coli* [pDmHhp], *E. coli* [pETDuet], or mixture of *E. coli* [pETmdh-His] and
173 *E. coli* [pEThps-phi] were suspended in 100 mM KPB (pH 6.5), 5 mM $MgCl_2$ and 100
174 mM F6P, to achieve an OD_{610} of 8.0, and incubated at 37°C. Methanol contained in the
175 purchased F6P (Sigma-Aldrich Japan K.K., Tokyo, Japan) was removed in advance by
176 dissolving F6P in 70% (v/v) acetonitrile and removing the solvent by a centrifugal
177 evaporator. For production of methanol from glucose, IPTG-induced *E. coli* [pDmHhp]
178 and *E. coli* [pETDuet] cells were suspended in 100 mM KPB (pH 6.5), 5 mM $MgCl_2$
179 and 2% (w/v) glucose, to achieve an OD_{610} of 10, and incubated at 37°C. In these
180 experiments, the reaction volume was 1 mL, and at each time point, 0.1 mL was

sampled, centrifuged at 20,000 x *g* for 2 min at 4°C, and the resulting supernatant was stored at 4°C. The methanol concentration in the supernatant was determined using a GC-2014 (Shimadzu Co, Kyoto, Japan) gas chromatograph equipped with a flame ionization detector and DB-1 column (30 m x 0.25 mm i.d. x 0.25 μm, Agilent Technologies, Santa Clara, CA, USA). Nitrogen gas was used as the carrier. The temperature program of the oven was 40°C for 5 min, then a ramp of 20°C min^{-1} to 200°C (held for 15 min), and the injector and detector were set at 250°C.

Results

Recombinant B. methanolicus S1 MDH catalyzes NADH-dependent reduction of formaldehyde to methanol both in vitro and in vivo

To confirm that recombinant MDH from *B. methanolicus* S1 catalyzes NADH-dependent reduction of formaldehyde to methanol as reported for the enzyme from *B. methanolicus* C1 [16], we constructed a T7 promoter-based expression vector for the NAD^+-dependent MDH gene (*mdh*) from *B. methanolicus* S1 tagged with 6xHis and introduced it into *E. coli* Rosetta (DE3). Although efficient methanol oxidation by the NAD^+-dependent MDH requires the activator protein Act, we did not express it because it is not required for the reverse reaction [16,22]. After production in *E. coli*, we purified MDH-His_6 using the Ni-NTA column (Figure S1). The specific activity of the purified MDH-His_6 to reduce formaldehyde to methanol with NADH was 10.0 units/mg at 37°C. This value was comparable to that of MDH purified from *B. methanolicus* C1 (19.6 units/mg at 50°C) [16] or the recombinant *E. coli* strain expressing the MDH gene of strain C1 (3.5 units/mg at 50°C) [23]. K_m and k_{cat} values for our purified MDH-His_6 at 37°C were 2.1 mM and 6.8 s^{-1}, respectively. Taken together, recombinant MDH from *B.*

205 *methanolicus* S1 can catalyze NADH-dependent reduction of formaldehyde to methanol
206 *in vitro*.
207 Next, we tested whether *E. coli* cells expressing MDH-His_6 can produce
208 methanol from formaldehyde in whole-cell reactions. After induction of *mdh*-His_6 by
209 IPTG, *E. coli* [pETmdh-His] cells were incubated in buffer containing 10 mM
210 formaldehyde at 37°C. The production of MDH-His_6 protein was confirmed by
211 immunoblot analysis (Figure S2). As a result, we observed an increase in the methanol
212 concentration in the reaction mixture, which was not observed with cells harboring
213 empty vector (*E. coli* [pET-23a(+)]) (Figure 2). Therefore, *E. coli* cells producing
214 recombinant MDH from *B. methanolicus* S1 can produce methanol from formaldehyde.
215 The methanol concentration after 41 h of incubation was 0.82 ± 0.02 mM.
216
217 ***Artificial fusion protein HPS-PHI catalyzes production of formaldehyde from F6P***
218 We next investigated whether the artificial fusion enzyme HPS-PHI derived from *M.*
219 *gastri* MB19 [20] catalyzes formaldehyde production from F6P. We used *E. coli*
220 [pEThps-phi] for production of the enzyme. Cell-free extract of IPTG-induced *E. coli*
221 [pEThps-phi] cells was prepared and subjected to enzyme assays. The specific activities
222 for forward (F6P production) and reverse (formaldehyde production) reactions were 2.0
223 ± 0.6 and (6.1 ± 0.1) x 10^{-1} units/mg, respectively. Neither enzyme activity was detected
224 with cells harboring empty vector (*E. coli* [pET-23a(+)]). The production of HPS-PHI
225 protein was confirmed by immunoblot analysis (Figure S3). Therefore, it was confirmed
226 that the artificial HPS-PHI can catalyze both the forward and reverse reactions as
227 reported for HPS-PHI from hyperthermophilic archaea [9,17].
228

Production of methanol from F6P through sequential reactions catalyzed by HPS-PHI and MDH

To test whether methanol can be produced from F6P through the sequential reactions catalyzed by HPS-PHI and MDH, we constructed a plasmid vector for co-expression of the genes encoding MDH-His_6 and HPS-PHI (pDmHhp), and introduced it into *E. coli* Rosetta (DE3). To confirm the co-expression of these genes, the cell-free extract of IPTG-induced *E. coli* [pDmHhp] cells was subjected to enzyme assays. Specific activities for formaldehyde reduction catalyzed by MDH at 37°C and for formaldehyde fixation catalyzed by HPS-PHI at 30°C were $(3.4 \pm 0.5) \times 10^{-2}$ and $(5.3 \pm 0.3) \times 10^{-1}$ units/mg, respectively. Neither enzyme activity was detected with cells harboring empty vector (*E. coli* [pETDuet]). The co-production of MDH-His_6 and HPS-PHI proteins was confirmed by immunoblot analyses (Figure S4). Thus, we succeeded in co-expressing genes encoding these two enzymes.

Next, we tested whether cells expressing *mdh*-His_6 and *hps-phi* can produce methanol from F6P in resting cell reactions. IPTG-induced *E. coli* [pDmHhp] cells were incubated in buffer containing 100 mM F6P for 24 h at 37°C. Results showed that methanol accumulated up to 1.5 ± 0.1 mM in the reaction mixture (Figure 3(a)), which was not observed for *E. coli* [pETDuet] cells (Figure 3(a)) or in the absence of F6P (data not shown). Thus, *E. coli* cells co-expressing *mdh*-His_6 and *hps-phi* could produce methanol from F6P. On the other hand, 20 ± 3 μM methanol was detected with *E. coli* [pETmdh-His] cells alone (Figure 3(a), 100% *E. coli* [pETmdh-His]). Nevertheless, the amount of methanol was about 75-fold lower than that by the co-expressing cells. In addition, methanol was not detected with *E. coli* [pEThps-phi] cells (Figure 3(a), 0% *E. coli* [pETmdh-His]). Collectively, efficient production of methanol was confirmed to

require both MDH-His_6 and HPS-PHI. We also tested the mixture of *E. coli* [pETmdh-His] and *E. coli* [pEThps-phi] cells, expecting that methanol could be produced by *E. coli* [pETmdh-His] cells from formaldehyde produced by *E. coli* [pEThps-phi] cells. However, the amount of methanol produced was less than that with the co-expressing cells with all of the mixing ratios tested (Figure 3(a)). This result shows that both enzymes should be produced in the same cell for efficient methanol production. This may be because formaldehyde was converted to methanol before formaldehyde induced the endogenous glutathione-dependent formaldehyde oxidation pathway in the co-expressing cells [24,25]. With *E. coli* [pDmHhp] cells, the methanol concentration reached 2.0 ± 0.01 mM after 72 h of incubation (Figure 3(b)).

Production of methanol from glucose by E. coli expressing mdh and hps-phi

Finally, we tested whether glucose could serve as a substrate for methanol production. Theoretically, glucose incorporated into *E. coli* cells is metabolized in glycolysis, producing as an intermediate F6P, the substrate for methanol production by MDH and HPS-PHI. We suspended *E. coli* [pDmHhp] cells in buffer containing 2% (w/v) glucose, and incubated them at 37°C. We observed the accumulation of methanol that was not observed with the *E. coli* [pETDuet] cells (Figure 4). With the *E. coli* [pDmHhp] cells, methanol accumulated up to 0.25 ± 0.02 mM after 72 h of incubation. As described above, methanol was not produced in the absence of substrate. Taken together, methanol was produced from glucose with the two heterologous enzymes.

Discussion

In this study, we established a novel pathway to produce methanol from F6P or glucose in *E. coli* cells via "reversed methylotrophy" by co-expression of genes encoding an NAD^+-dependent MDH and an artificial fusion protein HPS-PHI. These enzymes have been used to confer synthetic methylotrophy to non-methylotrophic microorganisms [10-15], but we confirmed that these enzymes can catalyze the reverse reactions of C1 metabolism both *in vitro* and *in vivo*, and successfully conferred reversed methylotrophy to *E. coli* (Figure 1).

The molar yield of methanol from formaldehyde by *E. coli* expressing *mdh* was 8.2% (Figure 2). Methanol was likely to have accumulated due to the absence of the MDH activator protein Act, which accelerates the undesired methanol oxidation reaction. Better yield may be achieved by eliminating the endogenous formaldehyde detoxification pathway [24,25]. Next, the molar yield of methanol from F6P by *E. coli* coexpressing *mdh* and *hps-phi* was 2.0% (Figure 3(b)). This low yield can be ascribed to the low expression level of the endogenous sugar phosphate-uptake system [26] or inactivation of MDH-His_6 and HPS-PHI, whose expression was not induced during the incubation with F6P. Finally, the molar yield of methanol from glucose was 0.23% (Figure 4), which was less than that from F6P. The yield may be improved by promoting glucose incorporation or engineering sugar metabolism to increase intracellular concentration of F6P, the substrate for methanol production by MDH and HPS-PHI. In this study, we did not attempt the production of methanol during growth on glucose because we adopted the pET vector system, whose promotor for the gene of interest is repressed in the presence of glucose. The use of a glucose non-repressible promoter will be suitable for methanol production accompanied by the growth on glucose. In spite of

the low yield of methanol from glucose, we succeeded in endogenous supply of methanol within the host cells, which has the potential to be utilized for bioproduction of useful compounds that need a methoxy group donor. For example, the supply of methanol is necessary for alcohol acyltransferase-catalyzed production of methyl short-chain esters (methyl acrylate, methyl methacrylate, and other methylester derivatives), which can be used as solvent, plasticizer or lubricant [27]. In such situations, methanol is usually supplied exogenously, however, introducing an endogenous production pathway for methanol and its use as the enzyme substrate within host cells would obviate the need for the exogenous supply and simplify the production process.

Because F6P is a ubiquitous metabolic intermediate, the substrate for methanol production can be expanded to other biomass-derived sugars, photosynthetic products, etc. Therefore, this work provides a versatile concept for the biological production and intracellular supply of methanol from various types of substrates that is useful for the production of industrial chemicals including methylesters. Furthermore, this concept is expected to be extended to bioindustrial production of methanol, a promising feedstock, from biomass.

Acknowledgements

This research was supported in part by JSPS KAKENHI, Grant Numbers JP25281063, JP16H02997, and JP19H04326.

Authors' contributions

The experiments were designed by T.T., Y.S., and H.Y. The experiments were performed by T.T., M.Y., D.H., and K.F. The data was analyzed by T.T., M.Y., D.H., K.F., Y.S., and

H.Y. The manuscript was written by T.T., Y.S., and H.Y.

Disclosure statement

No potential conflict of interest was reported by the authors.

References

1. Olah GA, Goeppert A, Prakash GS. Beyond oil and gas: the methanol economy, 2nd edn. Wiley-VCH, Weinheim; 2009.
2. Ochsner AM, Sonntag F, Buchhaupt M, et al. *Methylobacterium extorquens*: methylotrophy and biotechnological applications. Appl Microbiol Biotechnol. 2015;99:517-534.
3. Trotsenko YA, Torgonskaya ML. Current trends in methylotrophy-based biotechnology. Adv Biotechnol Microbiol. 2018;9:555763.
4. Schrader J, Schilling M, Holtmann D, et al. Methanol-based industrial biotechnology: current status and future perspectives of methylotrophic bacteria. Trends Biotechnol. 2009;27:107-115.
5. Keltjens JT, Pol A, Reimann J, et al. PQQ-dependent methanol dehydrogenases: rare-earth elements make a difference. Appl Microbiol Biotechnol. 2014;98:6163-6183.
6. Hektor HJ, Kloosterman H, Dijkhuizen L. Nicotinoprotein methanol dehydrogenase enzymes in Gram-positive methylotrophic bacteria. J Mol Catal, B Enzym. 2000;8:103-109.
7. Arfman N, Hektor HJ, Bystrykh LV, et al. Properties of an NAD(H)-containing methanol dehydrogenase and its activator protein from *Bacillus methanolicus*.

Eur J Biochem. 2004;244:426-433.

8. Chistoserdova L. Modularity of methylotrophy, revisited. Environ Microbiol. 2011;13:2603-22.

9. Orita I, Sato T, Yurimoto H, et al. The ribulose monophosphate pathway substitutes for the missing pentose phosphate pathway in the archaeon *Thermococcus kodakaraensis*. J Bacteriol. 2006;188:4698-4704.

10. Müller JEN, Meyer F, Litsanov B, et al. Engineering *Escherichia coli* for methanol conversion. Metab Eng. 2015;28:190-201.

11. Witthoff S, Schmitz K, Niedenführ S, et al. Metabolic engineering of *Corynebacterium glutamicum* for methanol metabolism. Appl Environ Microbiol. 2015;81:2215.

12. Meyer F, Keller P, Hartl J, et al. Methanol-essential growth of *Escherichia coli*. Nat Commun. 2018;9:1508.

13. Tuyishime P, Wang Y, Fan L, et al. Engineering *Corynebacterium glutamicum* for methanol-dependent growth and glutamate production. Metab Eng. 2018;49:220-231.

14. Woolston BM, King JR, Reiter M, et al. Improving formaldehyde consumption drives methanol assimilation in engineered *E. coli*. Nat Commun. 2018;9:2387.

15. Woolston BM, Roth T, Kohale I, et al. Development of a formaldehyde biosensor with application to synthetic methylotrophy. Biotechnol Bioeng. 2017;115:206-215.

16. Arfman N, Watling EM, Clement W, et al. Methanol metabolism in thermotolerant methylotrophic *Bacillus* strains involving a novel catabolic NAD-dependent methanol dehydrogenase as a key enzyme. Arch Microbiol.

1989;152:280-8.

17. Kato N, Yurimoto H, Thauer RK. The physiological role of the ribulose monophosphate pathway in bacteria and archaea. Biosci Biotechnol Biochem. 2006;70:10-21.

18. Yurimoto H, Hirai R, Yasueda H, et al. The ribulose monophosphate pathway operon encoding formaldehyde fixation in a thermotolerant methylotroph, *Bacillus brevis* S1. FEMS Microbiol Lett. 2002;214:189-193.

19. Arfman N, Dijkhuizen L, Kirchhof G, et al. *Bacillus methanolicus* sp. nov., a new species of thermotolerant, methanol-utilizing, endospore-forming bacteria. Int J Syst Bacteriol. 1992;42:439-445.

20. Orita I, Sakamoto N, Kato N, et al. Bifunctional enzyme fusion of 3-hexulose-6-phosphate synthase and 6-phospho-3-hexuloisomerase. Appl Microbiol Biotechnol. 2007;76:439-445.

21. Bradford MM. A rapid and sensitive method for the quantitation of microgram quantities of protein utilizing the principle of protein-dye binding. Anal Biochem. 1976;72:248-254.

22. Arfman N, Van Beeumen J, De Vries GE, et al. Purification and characterization of an activator protein for methanol dehydrogenase from thermotolerant *Bacillus* spp. J Biol Chem. 1991;266:3955-60.

23. de Vries GE, Arfman N, Terpstra P, et al. Cloning, expression, and sequence analysis of the *Bacillus methanolicus* C1 methanol dehydrogenase gene. J Bacteriol. 1992;174:5346-5353.

24. Gonzalez CF, Proudfoot M, Brown G, et al. Molecular basis of formaldehyde detoxification. Characterization of two *S*-formylglutathione hydrolases from

Escherichia coli, FrmB and YeiG. J Biol Chem. 2006;281:14514-14522.

25. Gutheil WG, Holmquist B, Vallee BL. Purification, characterization, and partial sequence of the glutathione-dependent formaldehyde dehydrogenase from *Escherichia coli*: a class III alcohol dehydrogenase. Biochemistry. 1992;31:475-481.

26. Weston LA, Kadner RJ. Role of *uhp* genes in expression of the *Escherichia coli* sugar-phosphate transport system. J Bacteriol. 1988;170:3375.

27. Kruis AJ, Bohnenkamp AC, Patinios C, et al. Microbial production of short and medium chain esters: Enzymes, pathways, and applications. Biotechnol Adv. 2019;37:107407.

Figure legends

Figure 1. Schematic diagram of the reversed methylotrophic pathway to produce methanol from F6P or glucose in recombinant *E. coli* cells. Solid arrows indicate reverse reactions of methanol oxidation and formaldehyde fixation via MDH and the RuMP pathway, respectively. Dashed arrows indicate endogenous metabolic pathways in *E. coli*. G6P, glucose 6-phosphate; F6P, fructose 6-phosphate; Ru5P, ribulose 5-phosphate; Hu6P, D-arabino-3-hexulose 6-phosphate; HPS, 3-hexulose-6-phosphate synthase; PHI, 6-phospho-3-hexuloisomerase; MDH, methanol dehydrogenase; PPP, non-oxidative pentose phosphate pathway.

Figure 2. Production of methanol from formaldehyde in a whole-cell reaction of *E. coli* expressing *mdh*-His_6. IPTG-induced *E. coli* [pET-23a(+)] (open circles) and *E. coli* [pETmdh-His] (closed circles) cells were suspended in a reaction mixture containing 10 mM formaldehyde and incubated at 37°C for the indicated time. The mean ± s.d. of triplicate incubations are shown. FRD activity of the cell-free extracts of *E. coli* [pET-23a(+)] and *E. coli* [pETmdh-His] cells used in this experiment were not detected and $(1.3 \pm 0.1) \times 10^{-2}$ units/mg at 37°C, respectively. The production of MDH-His_6 protein was confirmed by immunoblot analysis (Figure S2).

Figure 3. Production of methanol from F6P in whole-cell reactions of *E. coli* expressing *mdh*-His_6 and *hps-phi*. (a) Methanol production by *E. coli* [pETDuet] cells (EV), *E. coli* [pDmHhp] cells (co-exp.) or the mixtures of *E. coli* [pETmdh-His] and *E. coli* [pEThps-phi] cells at different ratios. IPTG-induced cells were suspended in a reaction mixture containing 100 mM F6P and incubated at 37°C for 24 h. n.d., not determined. (b) Time-

course of methanol production by *E. coli* [pETDuet] cells (open circles) and *E. coli* [pDmHhp] (closed circles). Reaction conditions and the analytical method were the same as in (a), and the cells were incubated for the indicated time. The mean ± s.d. of triplicate incubations are shown.

Figure 4. Production of methanol from glucose by *E. coli* expressing *mdh*-His_6 and *hps-phi*. IPTG-induced *E. coli* [pETDuet] (open circles) and *E. coli* [pDmHhp] (closed circles) cells were suspended in the buffer containing 2% (w/v) glucose to an OD_{610} 10, and incubated at 37°C for the indicated time. The mean ± s.d. of triplicate incubations are shown. For the samples with the *E. coli* [pETDuet] cells before 96 h, the concentrations of methanol were not determined.

Table 1. *E. coli* strains used in this study.

E. coli strain	Relevant characteristic(s)	Source
Rosetta (DE3)	F^- *ompT hsdS*$_B$($r_B^-m_B^-$) *gal dcm* (DE3) pRARE (Cam^R)	Novagen
Rosetta (DE3) [pET-23a(+)]	Rosetta (DE3) harboring pET-23a(+)	This study
Rosetta (DE3) [pETmdh-His]	Rosetta (DE3) harboring pETmdh-His	This study
Rosetta (DE3) [pEThps-phi]	Rosetta (DE3) harboring pEThps-phi	[20]
Rosetta (DE3) [pETDuet]	Rosetta (DE3) harboring pETDuet-1	This study
Rosetta (DE3) [pDmHhp]	Rosetta (DE3) harboring pDmHhp	This study

Table 2. Plasmids used in this study.

Plasmid	Relevant characteristic(s)	Source
pBluescript II SK(+)	Cloning vector	Stratagene
pBSmdh	pBluescript II SK(+) derivative; *mdh* from *B. methanolicus* S1 without the stop codon	This study
pET-23a(+)	T7 promoter-based expression vector	Novagen
pETmdh-His	pET-23a(+) derivative; *mdh* from *B. methanolicus* S1 in frame with C-terminal 6xHis-tag	This study
pEThps-phi	pET-23a(+) derivative; *hps-phi*	[20]
pETDuet-1	T7 promoter-based expression vector for two genes	Novagen
pDmH	pETDuet-1 derivative; *mdh*-His_6 from pETmdh-His in one of the two multiple cloning sites	This study
pDmHhp	pDmH derivative; *hps-phi* in the other multiple cloning site	This study

Table 3. Oligonucleotide primers used in this study.

Primer	Sequence (5'-3')	Purpose
mdh-fw-NheI	CTAGCTAGCATGACAAA CTTTTTCATTCC	Amplification of *mdh* gene excluding the stop codon from the genomic DNA of *B. methanolicus* S1 for construction of pBSmdh
mdh-rv-HindIII(Histag)	CCCAAGCTTCAGAGCG TTTTTGATGATTT	
mdh-fw-NcoI	CATGCCATGGGCATGAC AAACTTTTTCATTCC	Amplification of *mdh*-His_6 from pETmdh-His for construction of pDmH
mdh-His-rv-EcoRI	GGAATTCTCAGTGGTGG TGGTGGTGGTGCT	
MhMp-BglII	GAAGATCTCATGAAGCT CCAAGTCTCCAT	Amplification of *hps-phi* from pEThps-phi for construction of pDmHhp
MhMp-KpnI	GGGGTACCTCACTCGA GGTTGGCGTGGCGCG	

Fig. 1

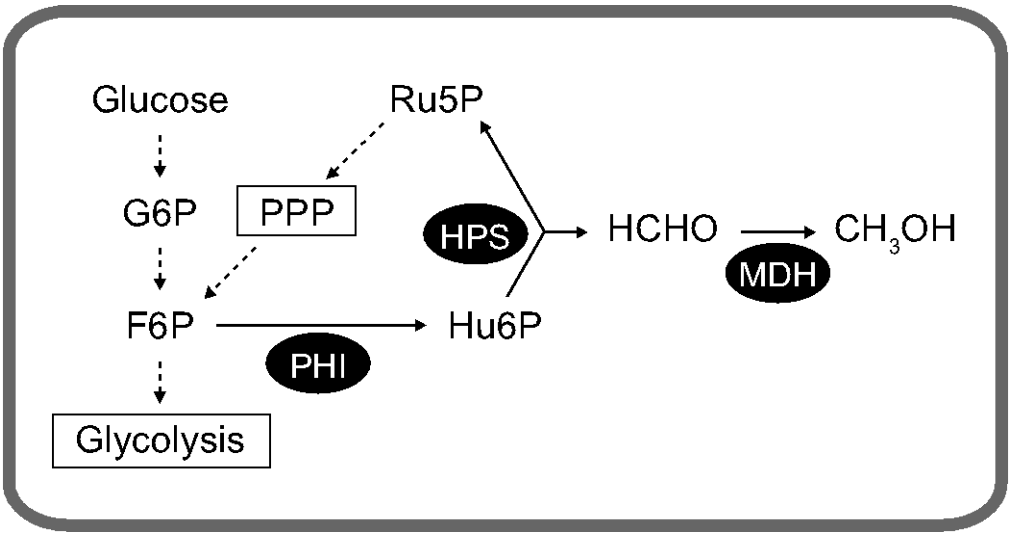
Glucose
Ru5P
G6P
PPP
HPS
HCHO
CH_3OH
MDH
F6P
Hu6P
PHI
Glycolysis

Fig. 2

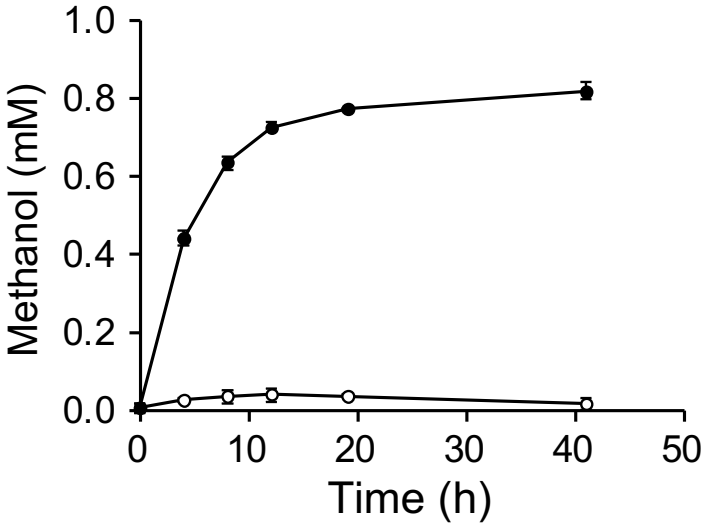

Fig. 3

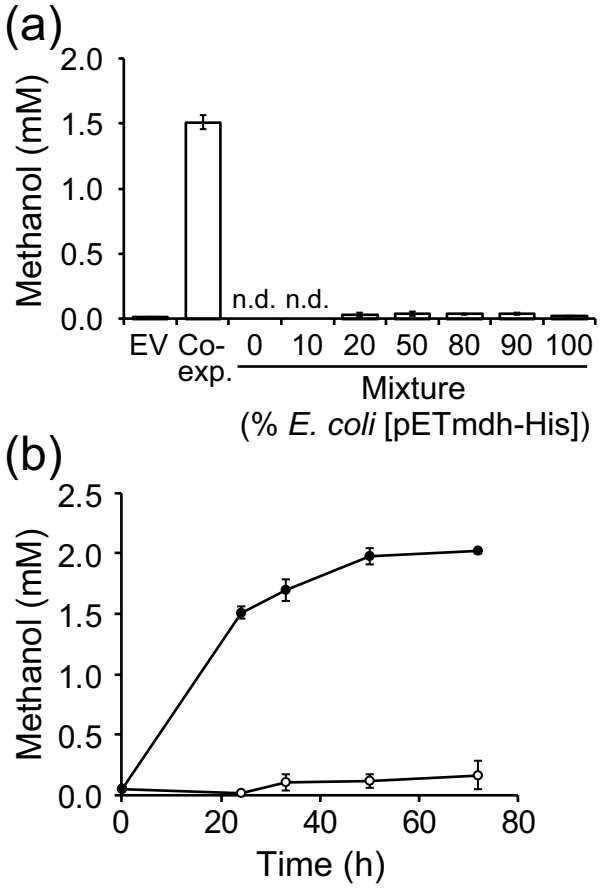
(a)
Methanol (mM)
2.0
1.5
1.0
0.5
0.0
n.d. n.d.
EV
Co-exp.
0
10
20
50
80
90
100
Mixture
(% E. coli [pETmdh-His])
(b)
Methanol (mM)
2.5
2.0
1.5
1.0
0.5
0.0
0
20
40
60
80
Time (h)

Fig. 4

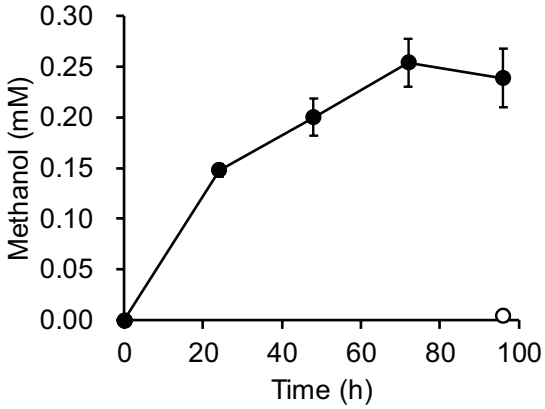

Supplementary information

Methanol production by reversed methylotrophy constructed in *Escherichia coli*

Tomoyuki Takeya, Miyabi Yamakita, Daisuke Hayashi, Kento Fujisawa, Yasuyoshi Sakai, and Hiroya Yurimoto*

Division of Applied Life Sciences, Graduate School of Agriculture, Kyoto University, Kitashirakawa-Oiwake, Sakyo-ku, Kyoto 606-8502, Japan

*Correspondence: Hiroya Yurimoto, Division of Applied Life Sciences, Graduate School of Agriculture, Kyoto University, Kitashirakawa-Oiwake, Sakyo-ku, Kyoto 606-8502, Japan. Tel.: +81 75 753 6387; Fax: +81 75 753 6454; E-mail: yury@kais.kyoto-u.ac.jp

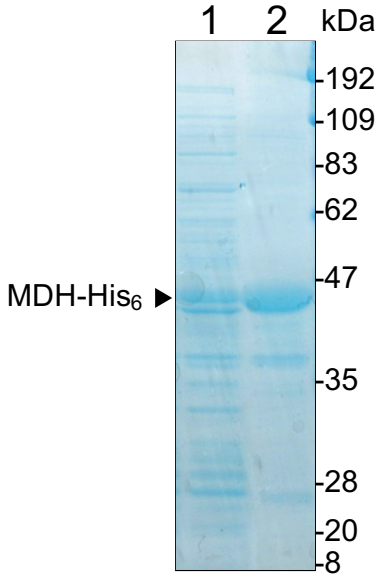

Figure S1. SDS-PAGE analysis of the protein production and purification of recombinant MDH tagged with 6xHis (MDH-His_6) using a Ni-NTA column. Lane 1, Cell-free extract of *E. coli* [pETmdh-His]. Lane 2, Imidazole elution of MDH-His_6 from the Ni-NTA column. The theoretical molecular mass of MDH-His_6 is 42 kDa.

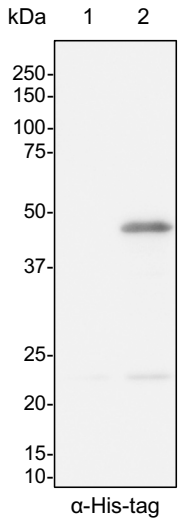

Figure S2. Immunoblot analysis of MDH-His_6 protein in the cell-free extracts of the cells used in Fig. 2. Lane 1, *E. coli* [pET-23a(+)]. Lane 2, *E. coli* [pETmdh-His]. The size of the major band appeared in lane 2 (42 kDa) agreed with that in lane 2 of Fig. S1, confirming the production of MDH-His_6 protein in the *E. coli* [pETmdh-His] cells.

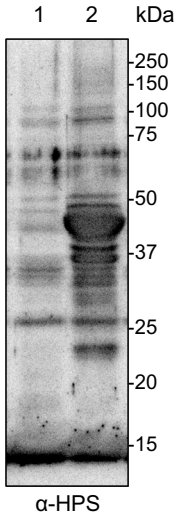

Figure S3. Immunoblot analysis of HPS-PHI protein in the cell-free extracts of *E. coli* [pET-23a(+)] (lane 1) and *E. coli* [pEThps-phi] (lane 2) cells. The size of the major band appeared in lane 2 (42 kDa) agreed with that of purified HPS-PHI observed previously [1], confirming the production of HPS-PHI protein in the *E. coli* [pEThps-phi] cells.

Reference

1. Orita I, Sakamoto N, Kato N, et al. Bifunctional enzyme fusion of 3-hexulose-6-phosphate synthase and 6-phospho-3-hexuloisomerase. Appl Microbiol Biotechnol. 2007;76:439-445.

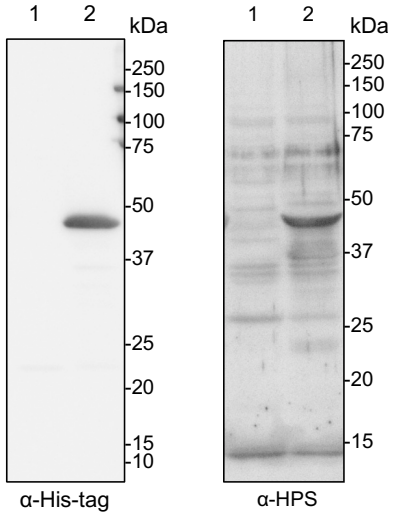

Figure S4. Immunoblot analyses of MDH-His_6 and HPS-PHI proteins in the cell-free extracts of *E. coli* [pETDuet] (lane 1) and *E. coli* [pDmHhp] (lane 2) cells. The sizes of the major bands appeared in lane 2 in α-His-tag and α-HPS-detections agreed with that of Fig. S2 and S3, respectively, confirming the co-production of MDH-His_6 and HPS-PHI proteins.